

# Characterization of chemically synthesized undoped and doped ZnS nanoparticles

Pawan Kumar Pathak

Department of Physics, SSV (PG) College, Hapur  
Chaudhary Charan Singh University, Meerut (U.P.) 250004, India

Subodh Kumar Sharma

Department of Physics, SSV (PG) College, Hapur  
Chaudhary Charan Singh University, Meerut (U.P.) 250004, India

---

## Abstract

This study presents a comprehensive analysis of the structural, morphological, and optical properties of undoped and doped ZnS nanoparticles synthesized via the chemical precipitation method. The crystallite sizes of the nanoparticles were calculated using Scherrer's equation, while phase identification was performed through X-Ray Diffraction (XRD). The analysis included undoped ZnS and ZnS nanoparticles doped with 2% of Ca, Mn, Co, Ni, and Ba, enabling a comparison of doping effects. Surface morphology was examined using Field Emission Scanning Electron Microscopy (FESEM), revealing insights into the nanoparticle size, shape, and distribution. The optical properties were studied using UV-Vis spectroscopy, focusing on the absorption spectra and band gap energy. The absorption spectra exhibited characteristic peaks in the range of 232–340 nm. The optical band gaps of the ZnS nanoparticles were found to decrease with doping, particularly with manganese. The direct band gap energy of the samples ranged from 4.46 eV for undoped ZnS to 3.87 eV for Mn-doped ZnS, indicating a significant influence of doping on the electronic structure. This systematic investigation highlights the potential for tailoring ZnS nanoparticle properties through controlled doping, making them suitable for various optoelectronic and photonic applications.

**Keywords:** ZnS nanoparticles; Field Emission Electron Microscope (FESEM) UV-Vis spectrophotometer, X-Ray diffraction (XRD)

---

Date of Submission: 10-04-2025

Date of Acceptance: 25-04-2025

---

## I. Introduction

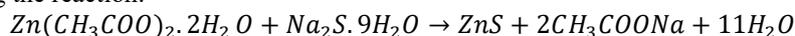
Zinc Sulphide (ZnS) is a prominent II-VI group inorganic semiconductor material, widely recognized for its exceptional optical and electronic properties. ZnS exhibits excellent transmission characteristics, with a refractive index of 2.27 at a wavelength of 1  $\mu\text{m}$  [1]. It is a wide-bandgap semiconductor that exists in two stable structural phases at 300 K: the cubic zinc blende phase and the hexagonal wurtzite phase [2, 3]. In recent years, there has been a growing interest in nanostructured materials, particularly nanostructured semiconductors, due to their remarkable physical and chemical properties compared to bulk materials. Nanostructured ZnS, in particular, exhibits unique features such as enhanced energy absorption, quantum confinement effects, and size-dependent bandgap variations, making it an attractive material for advanced technological applications [6]. A variety of methods have been developed for synthesizing semiconductor nanomaterials, each tailored to achieve specific properties and applications. This study focuses on the synthesis and characterization of undoped and Mn-doped ZnS nanoparticles prepared using the chemical precipitation method. Key aspects of the investigation include crystallite size determination using Scherrer's equation, phase identification through X-Ray Diffraction (XRD), morphological analysis of the samples using Field Emission Scanning Electron Microscopy (FESEM), optical characterization, including band gap determination via UV-Vis spectrophotometry and luminescence properties evaluated using a Fluorescence Spectrophotometer. ZnS is a highly versatile semiconductor nanomaterial with applications spanning electronics, optoelectronics, catalysis, and medicine [3]. Its notable bandgap and tunable properties make it particularly suitable for advanced technologies such as flat-panel displays and electroluminescent windows [5].

## II. Experimental

The samples were prepared using two methods: mechanochemical and chemical.

### 2.1 Mechanochemical Method

Zinc sulfide (ZnS) was synthesized by milling zinc acetate and sodium sulfide in a Retsch PM 400/2 planetary ball mill, following the reaction:



The powder was sealed in a steel jar with steel balls and milled at a ball-to-powder ratio of 5:1, a milling speed of 300 rpm, and a vial rotation speed of 600 rpm for 30–120 minutes. To remove impurities, the milled powder was treated with methanol using a Remi PR 24 centrifuge at 10,000 rpm for 5 minutes, followed by multiple methanol washes. The cleaned powder was then dried at 50°C for 2 hours and subjected to heat treatment at temperatures of 100°C, 200°C, 300°C, and 400°C for 1 hour each.

### 2.2 Chemical Method

Chemical precipitation was carried out at room temperature using zinc acetate, manganese acetate, and sodium sulfide. To synthesize the nanoparticles, 2.195 g of zinc acetate and 0.049 g of manganese acetate were dissolved in a solution and stirred for 15 minutes. Subsequently, 50 mL of 2.451 g sodium sulfide solution was added dropwise under vigorous stirring for 25 minutes, forming a dull white colloidal solution. Acrylic acid (AA) was introduced into the mixture and stirred for an additional 20 minutes. The resulting precipitate was separated, washed thoroughly with methanol, and dried at 50°C for 24 hours. After drying, the solid product was crushed into a fine powder using a mortar and pestle. Samples with varying manganese doping concentrations (4% and 6%) were prepared following the same procedure. All prepared powders were characterized after processing to evaluate their properties.

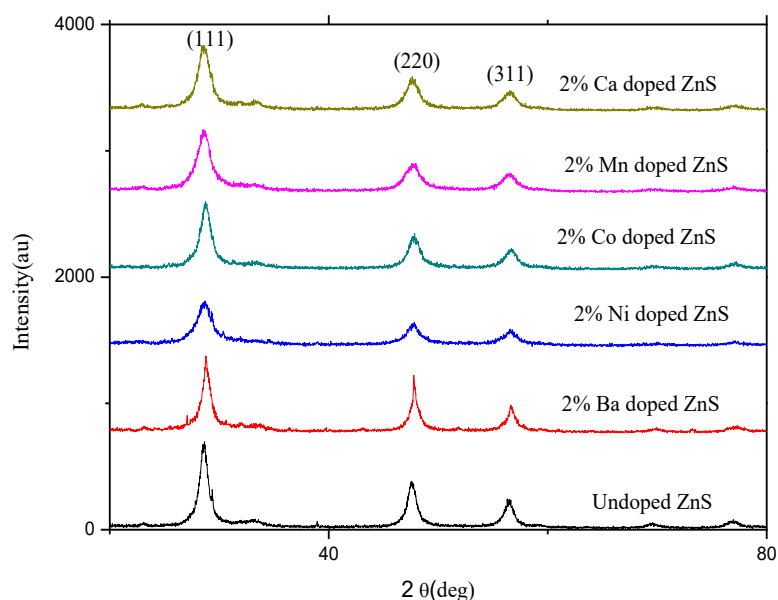
## III. Results and Discussion

### 3.1 X-ray diffraction pattern

XRD studies are an efficient tool for analyzing the structural properties of the samples. The size of all the samples are determined by Bruker AXS D8Advance X-ray diffractometer with CuK $\alpha$  radiation ( $\lambda=0.15406\text{nm}$ ) operating at 40 kV and 30 mA. XRD data are collected over the range 20-80 $^\circ$  at room temperature. The XRD patterns of undoped and doped ZnS nanoparticles are shown in Fig.(1) JCPDS Card No.5-566. The crystallite size can be calculated with the help of Scherrer's equation below

$$D = \frac{0.9\lambda}{\beta \cos \theta} \quad (1)$$

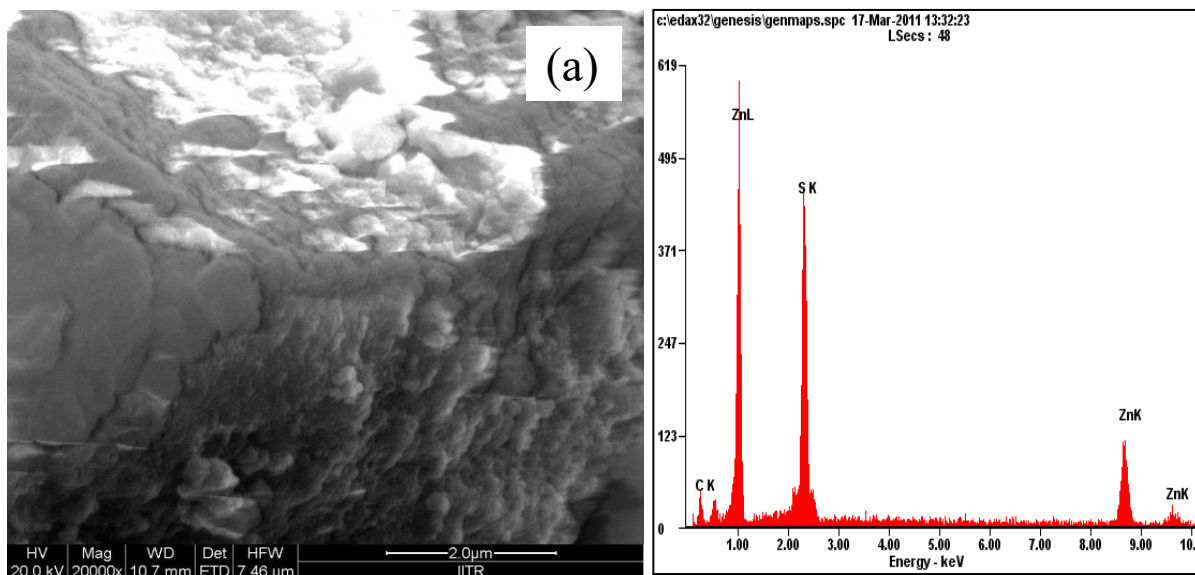
Where  $D$  is the mean grain size,  $\lambda$  is the X-ray wavelength (for CuK $\alpha$  radiation,  $\lambda = 0.15406 \text{ nm}$ ),  $\theta$  is the diffraction angle and  $\beta$  is full width at half maximum. The grain size of the undoped and doped ZnS nanoparticles calculated by using Eq.6.1 is in range of 6.10 - 8.30 nm shown in Table- 1. Fig.(1) shows the three diffraction peak at  $2\theta$  values 28.62 $^\circ$ , 47.64 $^\circ$ , 56.59 $^\circ$ . The peaks are appearing due to reflection from the (111), (220) and (311) planes of the cubic phase of the ZnS. The obtained peak positions correspond to zinc blended type patterns for all the samples. The XRD pattern of the nanocrystal is well matched with the Standard cubic ZnS [33]. In this investigation we found that with increasing amount of Acrylic acid (AA) grain size is decreasing as shown in Table-1

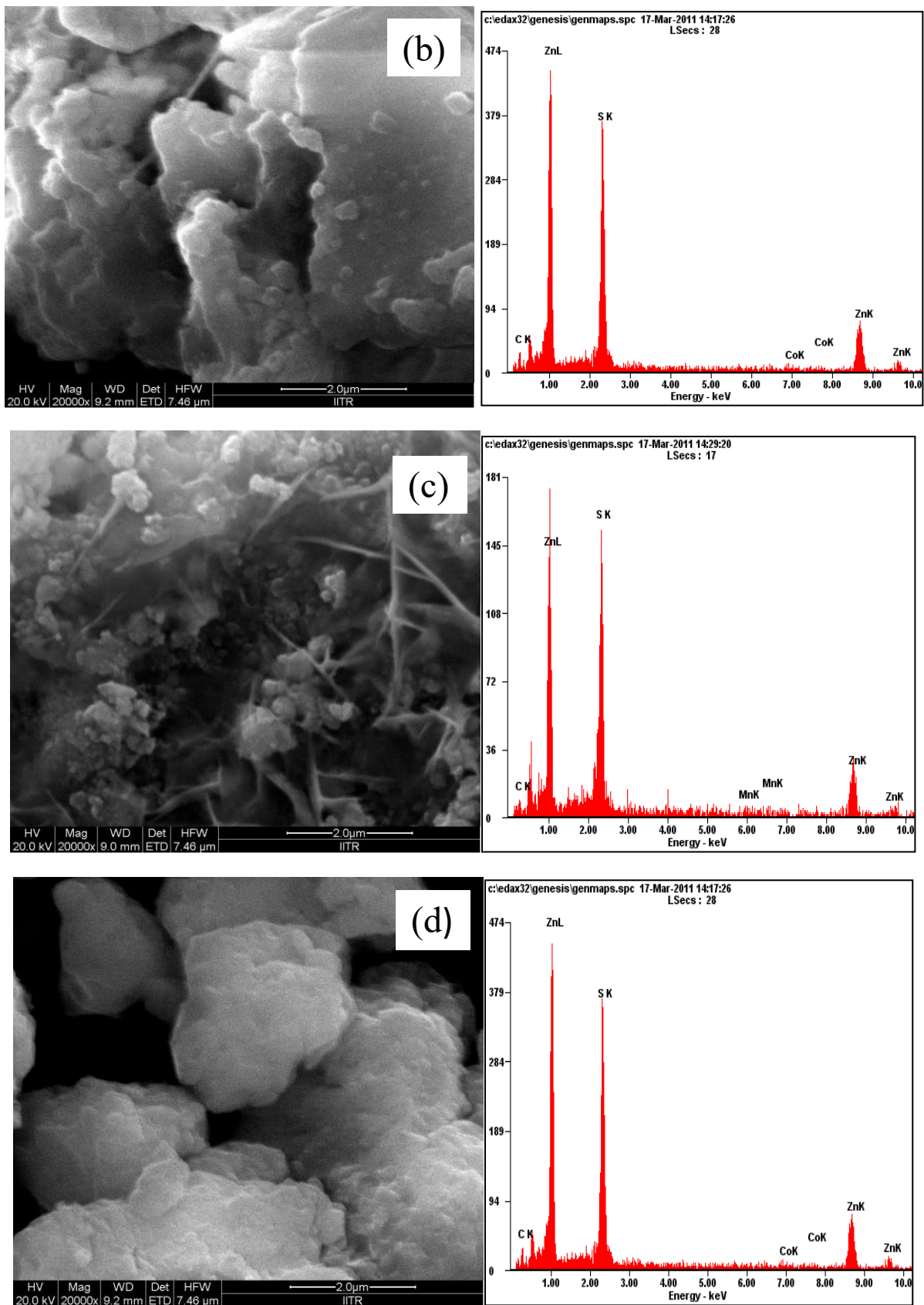


**Fig.(1)** XRD pattern of undoped and doped ZnS nanoparticles

### 3.2 SEM analyses

Fig. 2 shows SEM images of pure ZnS, 2% Ni doped, 2% Mn doped, 2% Co doped, 2% Ca doped and 2% Ba doped ZnS respectively and their corresponding EDAX which confirmed the composition of ZnS. From the SEM images, the formation of nanoparticles is clearly observed but the actual size of the nanoparticles cannot be determined from the FESEM images as it is limited by the resolution of the used FESEM instrument.





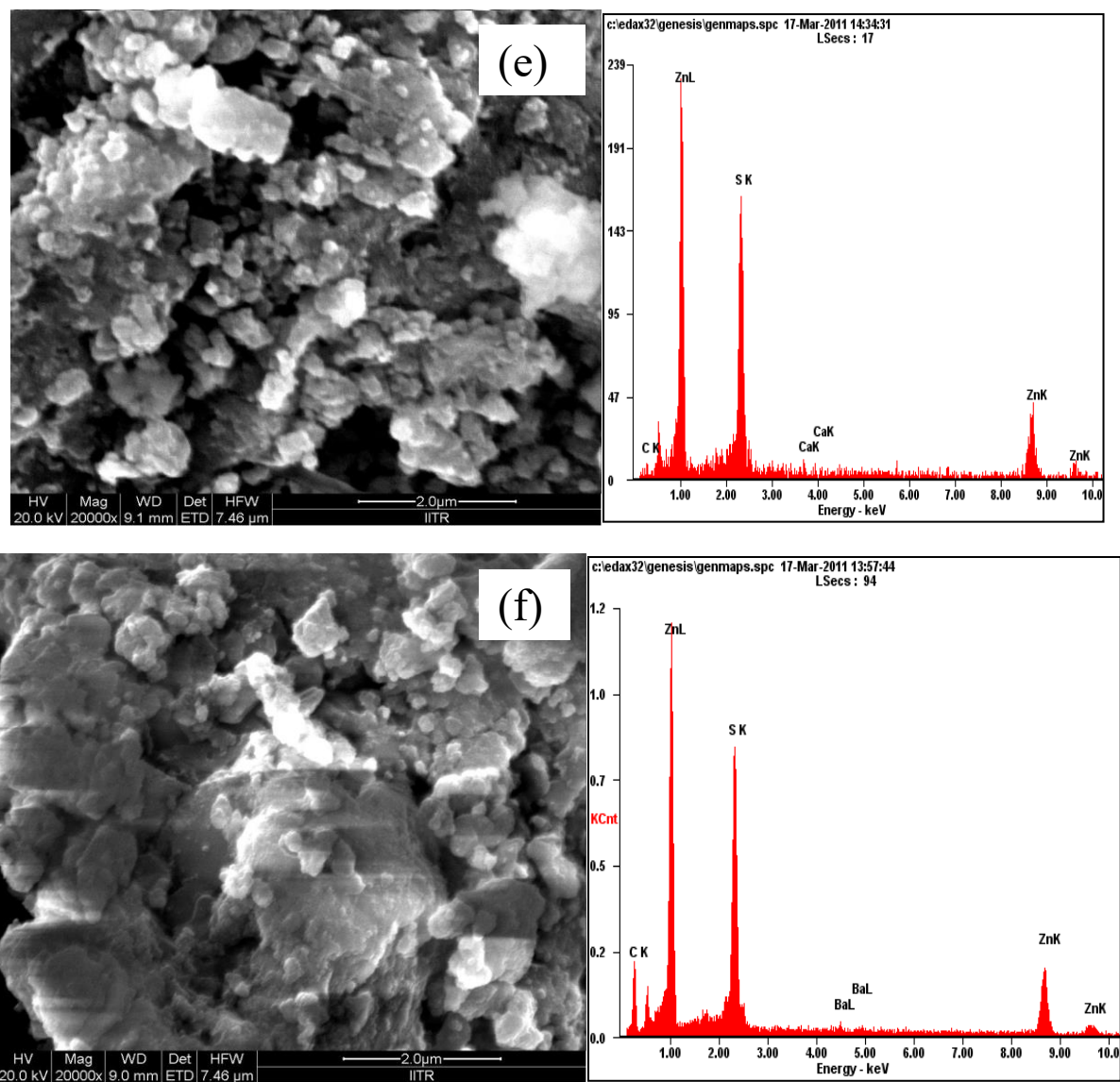


**Fig.2** FESEM images of (a) pure ZnS, (b) 2% Ni doped, (c) 2% Mn doped, (d) 2% Co doped, (e) 2% Ca doped and (f) 2% Ba doped ZnS respectively and their corresponding EDAX.

### 3.3 Optical absorption and band gap

The optical absorption spectra have been observed by using UV-Visible-NIR (Varian, Cary 5000) spectrophotometer and the results are shown in Fig.3 To measure the absorption characteristics, the synthesized ZnS nanopowders are first dispersed in methanol and then taken on a quartz cuvette. Optical absorption spectra of undoped and doped ZnS nanoparticles shows that the peak appears in the range of 330-250 nm. These peak positions reflect the band gap of nanoparticles and the synthesis ZnS nanoparticles have no absorption in the visible region (800-400nm).

The relation between the incident photon energy ( $h\nu$ ) and the absorption coefficient ( $\alpha$ ) is given by the following relation

$$(\alpha h\nu)^{\frac{1}{n}} = A(h\nu - E_g) \quad (2)$$

Where  $A$  is constant and  $E_g$  is the band gap energy of the material and the exponent  $n$  depends on the type of transition. For direct allowed transition  $n = 1/2$ , for indirect allowed transition  $n = 2$ , for direct forbidden  $n = 3/2$  and for indirect forbidden  $n = 3$ . Direct band gap of the samples are calculated by plotting  $(\alpha h\nu)^2$  verses  $h\nu$  and then extrapolating the straight portion of the curve on  $h\nu$  axis at  $\alpha = 0$  as shown in Fig.4 The band gap energy of the samples are indicated in Table-1. The obtained values of the band gap of ZnS and Mn doped ZnS nanoparticles are higher than that of the bulk value of ZnS (3.68 eV).

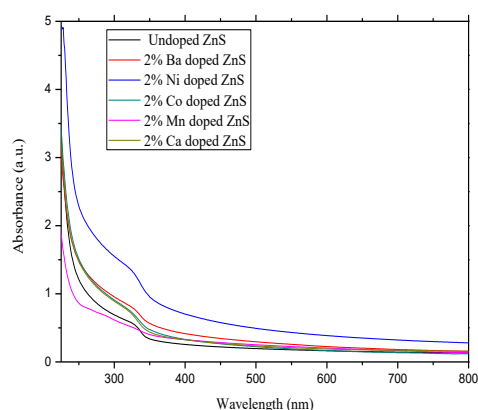


**Fig.3** Absorption spectrum of undoped and doped nanoparticles

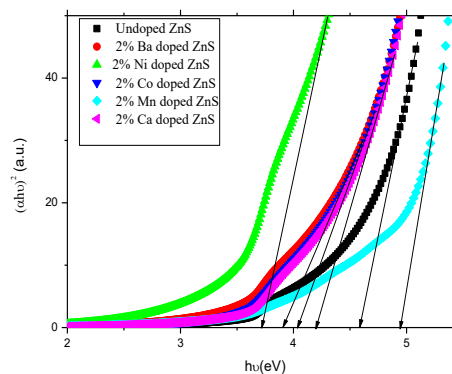


**Fig.4** Calculation of optical band from the ZnS UV-Vis-NIR absorption spectra

**Table 1. Crystallite size and corresponding band gap energy of the synthesis nanomaterials.**

Sample Name	Crystallite size (nm)	Band gap energy(eV)
Undoped ZnS	8.30	4.59
2% Ba doped ZnS	8.20	3.91
2% Ni doped ZnS	6.10	3.73
2% Co doped ZnS	7.40	4.04
2% Mn doped ZnS	7.48	4.95

### 3.4 Photoluminescence study of ZnS and doped ZnS nanoparticles

The Photoluminescence (PL) of undoped and doped ZnS samples are measured at room temperature using F-2500 FL Spectrophotometer. The PL emission spectra obtained at 310 nm excitation of undoped ZnS and doped ZnS with different doping elements are shown in Fig.5 It is observed that PL emission band from undoped ZnS nanoparticles are highly asymmetric and broaden with multiple peaks in blue region. Peaks are found at 426, 438 and 444 nm. ZnS samples doped with 2% Ba<sup>2+</sup> shows emission peak at 426 and 448 nm. Ni<sup>2+</sup> ions occupy the Zn<sup>2+</sup> ions in the ZnS crystal acting as trapping sites. In the PL process, an electron from the ZnS valence band is excited across the band gap and photo excited electron subsequently decays by a normal recombination process to some surface or defect states [19]. Ni<sup>2+</sup> doped ZnS samples shows emission at 426, 448 and 485 nm. Co<sup>2+</sup> doped ZnS samples shows emission at 426, 445 and 486 nm. Co<sup>2+</sup> is acting as a sensitizing agent and so the radiative recombination processes are enhanced [20]. Thus, PL intensity of Co doped ZnS sample are higher than those of undoped ZnS sample. The PL spectrum of Mn<sup>2+</sup> doped ZnS nanoparticles shows the efficient emission of orange color light with peak at 594 nm. The Mn<sup>2+</sup> ion has a 3d<sup>5</sup> configuration. The Mn<sup>2+</sup> ion exhibits a broad emission peak. Mn<sup>2+</sup> d-electron states act as efficient luminescent centers while interacting with s-p state of the ZnS host The subsequent transfer of electron and hole pairs in to the electronic level of the Mn<sup>2+</sup> ion leads to the orange emission from the <sup>4</sup>T<sub>1</sub>-<sup>6</sup>A<sub>1</sub> transition .The emission takes place via energy transfer from the excited state of the ZnS host lattice to the d electrons of Mn<sup>2+</sup>. Ca<sup>2+</sup> doped ZnS nanoparticles shows emission at 426,448 and 485 nm in visible region.

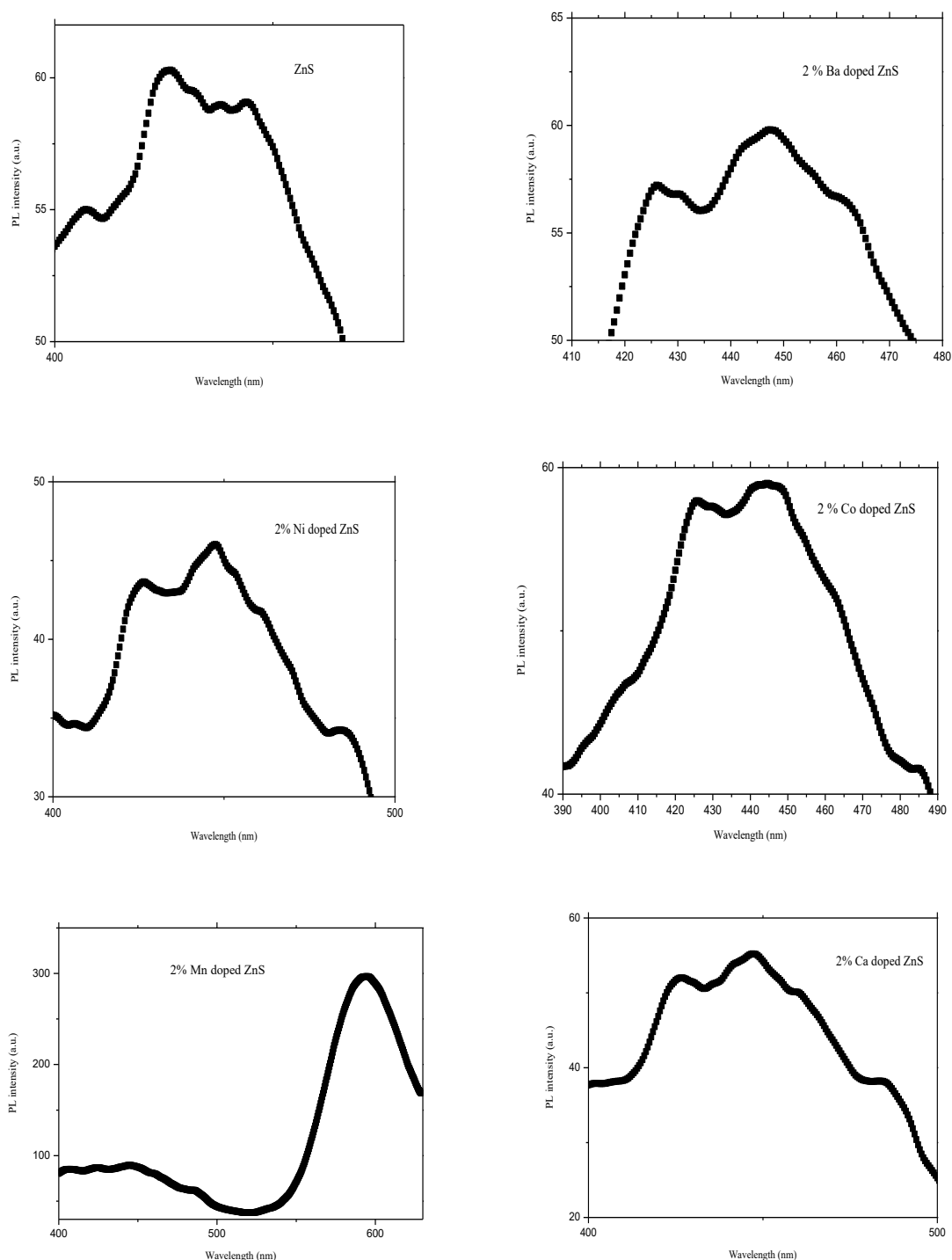


**Fig.5** Show the PL emission from the undoped ZnS and doped (Ba, Ni, Co, Mn and Ca) ZnS nanoparticles

#### IV. Conclusions:

In summary, this study provides a detailed investigation into the structural, morphological, and optical properties of undoped and doped ZnS nanoparticles synthesized via the chemical precipitation method. The results demonstrate that doping significantly influences the crystallite size, surface morphology, and optical properties of ZnS nanoparticles. XRD analysis confirmed phase formation, while FESEM revealed variations in morphology due to doping. UV-Vis spectroscopy showed that the absorption peaks of the nanoparticles occurred within the range of 232–340 nm, with the direct band gap energy decreasing from 4.46 eV for undoped ZnS to 3.87 eV for Mn-doped ZnS. This decrease in band gap with doping, particularly with manganese,

highlights the potential to tune the electronic and optical properties of ZnS nanoparticles. The findings underscore the versatility of ZnS nanoparticles for tailored applications in optoelectronic and photonic devices through controlled doping strategies.

#### **Conflict of interest**

The authors confirm that there is no conflict of interest to declare for this publication.

#### **Acknowledgements**

This research did not receive any specific grant from funding agencies in public, commercial, or not-for-profit sectors. The authors would like to thank the editor and anonymous reviewers for their comments that help to improve the quality of this work.

#### **References:**

- [1] Prayas Chandra Patel, Neelabh Srivastava, P. C. Srivastava, Synthesis of Wurtzite ZnS Nanocrystals at low temperature, *J Mater Sci: Mater Electron*, (2013), s10854-013-1367. <http://dx.doi.org/10.1007/s10854-013-1367-z>
- [2] S. Senthilkumar and R. Thamiz Selvi, Formation and Photoluminescence of Zinc Sulphide Nanorods, *Journal of Applied Sciences*, 8(12): 2306-2311, 2008. <https://doi.org/10.3923/jas.2008.2306.2311>
- [3] Tran Thi Quynh Hoa, Le Van, Ta Dinh Canh and Nguyen Ngoe Long, Preparation of ZnS nanoparticles by hydrothermal method, *Journal of Physics, Conference Series* 187 (2009) 012081.
- [4] J. F. Xu, W. Ji, J. Y. Lin, S. H. Tang, Y. W. Du, Preparation of ZnS nanoparticles by ultrasonic radiation method, *Applied Physics A*, 66, 693-641 (1998).
- [5] X. M. Meng, J. Liu, Y. Jiang, W. W. Chen, C. S. Lee, I Bello, S. T. Lee, Structure and size-controlled ultrafine ZnS nanowires, *Chemical Physics Letters*, 382 (2003) 434-438. <https://doi.org/10.1016/j.cplett.2003.10.093>
- [6] Khalid T. Al-Rasoul, Nada K. Abbas, Zainb J. Shanan, Structural and optical characterization of Cu, and Ni doped ZnS nanoparticles, *Int. J. Electrochem. Sci.* 8 (2013) 5594-6504. [http://dx.doi.org/10.1016/S1452-3981\(23\)14706-7](http://dx.doi.org/10.1016/S1452-3981(23)14706-7)
- [7] J. H. Park, J. Y. Kim, B. D. Chin, Y. C. Kim, and O. O. Park, *Nanotechnology* 15, (2004) 1217.
- [8] N. Karar, F. Singh, B. R. Mehta, *J. Appl. Phys.* 95, (2004), 656.
- [9] P. Balaz, M. Balintova, Z. Bastl, J. Briancin, V. Sepelak, *Solid State Ionics* 101-103(1997) 45-51.
- [10] P. Balaz, E. Boldizarova, E. Godocikova, J. Briancin, *Materials Letters* 57(2003) 1585-1589.
- [11] Erika Godocikova, Peter Balaz, Eberhard Gock, Woo Sik Choi, Byung Sun Kim, *Powder Technology* 164(2006) 147-152.
- [12] T. Tsuzuki, J. Ding, P. G. McCormick, *Physica B* 239(1997)378-387.
- [13] R. N. Bhargava, D. Gallagher, X. Hong, A. Nurmikko, *Phys. Rev. Lett.* 72 (1994) 416.
- [14] S. W. Lu, B. I. Lee, Z. L. Wang, W. Tong, B. K. Wagner, W. Park, C. J. Summers, *J. of Luminescence*, 92 (2001).
- [15] P. K. Ghosh, Sk. F. Ahmed, S. Jana, K. K. Chattopadhyay, *Optical Materials* 29 (2007) 1584-1590. <https://doi.org/10.1016/j.optmat.2006.07.016>
- [16] S. K. Mandal, A. R. Mandal, S. Das, B. Bhattacharjee, *J. Appl. Phys.* 101 (2007) 114315.
- [17] M. Zalewska, B. Kuklinski, E. Grzanka, S. Malik, J. Jezierska, B. Palosz, M. Grinberg, A. M. Klonkowski, *Journal of Luminescence*. 129 (2009) 246.
- [18] M. Tanaka, *Journal of Luminescence*, 100 (2002) 163.
- [19] A. A. Khosravi, M. Kundu, B. A. Kuruvilla, G. S. Shekhawat, R. P. Gupta, A. K. Sharma, P. D. Vyas, S. K. Kulkarni, *Appl. Phys. Lett.* 67 (1995) 2506.
- [20] Hemant Soni, Mukesh Chawda, Dhananjay Bodas, *Materials Letters* 63 (2009) 767-769.
- [21] R. Sarkar, C. S. Tiwary, P. Kumbhakar, A. K. Mitra, *Physica B* 404 (2009) 3855-3858.
- [22] Greenwood, Norman N.; Earnshaw, A. (1984), *Chemistry of the Elements*, Oxford: Pergamon, p. 1405, ISBN 0-08-022057-6.
- [23] Kaelble E F, *Handbook of X-rays*, McGraw-Hill, New York, 1967.
- [24] B. D. Cullity and S. R. Stock, *Elements of X-Ray diffraction*, 3rd edition, prentice hall, upper Saddle River, NJ, 2001.
- [25] P. J. Grundy and G. A. Jones, "Electron Microscopy in the Study of Materials", (Edward Arnold Publishers Limited, (1976).
- [26] P. E. J. Flewitt, and R. K. Wild, "Physical Methods for Materials Characterization", Chapter 6, (IOP Publishing, Bristol, 1994).
- [27] E. Ivanov, C. Suryanarayana *J. of Materials Synthesis and Processing*, Vol 8 Nos 3/4, 2000.
- [28] P. Balaz, P. Pourghahramani, E. Dutkova, E. Turianicova, J. Kovac, A. Satka, *Phys. stat. sol. (c)* 5, No. 12, 3756-3758 (2008).
- [29] M. Zalewska, B. Kuklinski, E. Grzanka, S. Malik, J. Jezierska, B. Palosz, M. Grinberg, A. M. Klonkowski, *J. of Luminescence*, 129 (2009) 246.
- [30] W. Q. Peng, S. C. Qu, G. W. Cong, Z. G. Wang, *Journal of Crystal Growth* 279 (2005) 454-460.